PNAS
www.pnas.org

Supplementary Information for

Pathogenic Role of Delta 2 Tubulin in Bortezomib Induced Peripheral Neuropathy

Maria Elena Pero[a,b], Cristina Meregalli[c], Xiaoyi Qu[a,1], Grace Ji-eun Shin[d,e], Atul Kumar[a], Matthew Shorey[f], Melissa M. Rolls[f], Kurenai Tanji[a,g], Thomas H. Brannagan[g], Paola Alberti[c], Giulia Fumagalli[c], Laura Monza[c], Wesley B. Grueber[d,e], Guido Cavaletti[c], and Francesca Bartolini[a,*]

[a]Department of Pathology & Cell Biology, Columbia University Medical Center, 10032, New York, NY; [b]Department of Veterinary Medicine and Animal Production, University of Naples Federico II, 80137, Naples, Italy; [c]Experimental Neurology Unit, School of Medicine and Surgery and NeuroMI (Milan Center for Neuroscience), University of Milano-Bicocca, 20900, Monza, Italy; [d,e]Departments of Physiology and Cellular Biophysics and Neuroscience, Columbia University, Zuckerman Mind Brain and Behavior Institute, Jerome L. Greene Science Center, 10027, New York, NY; [f]Department of Biochemistry and Molecular Biology, Penn State University, 16802, University Park, PA; [g]Department of Neurology, Columbia University Medical Center, 10032, New York, NY; [1]new address: Genentech, Inc., 94080, South San Francisco, CA

*Corresponding author: Francesca Bartolini
Email: fb2131@columbia.edu

This PDF file includes:

Supplementary text
Figures S1 to S9 with their legends
Table S1
Legends for Movies S1 to S15
SI References

Other supplementary materials for this manuscript include the following:

Movies S1 to S15

Supplementary Information Text

Methods

Animals. *In vivo* experiments were carried out on female Wistar rats (Envigo, Udine, Italy), weighing between 175 and 200 g at the beginning of the experimental procedure (n=6-13 rats/group). The rats were housed under constant temperature and lighting conditions with a 12 h light/dark cycle and they received food and water *ad libitum*. Procedures and experimental protocols were compliant with the ethics guidelines described in national (DL. Vo 26/2014, Gazzetta Ufficiale della Repubblica Italiana, permit No1161/2016) and international laws (European Union Directive 2010/63/EU: Guide for the Care and Use of Laboratory Animals, U.S National Research Council, 1996). All the experiments were approved by the Italian State authorities (14/2016). For the *in vitro* experiments, all protocols and procedures used to prepare primary culture of DRG neurons dissected from wild type mice (C57BL/6) were approved by the Committee on the Ethics of Animal Experiments of Columbia University and in agreement with the Guide for the Care and Use of Laboratory Animals distributed by the National Institutes of Health.

Behavioral analysis and neurophysiology. At baseline, 24 h after a single Bort administration and 24 h after the chronic administration of the antineoplastic drug, a blinded examiner performed behavioral tests in random fashion in order to evaluate mechanical and thermal nociceptive thresholds through Dynamic and Plantar tests, respectively, as previously described (1). The Dynamic test used an algesimeter (Ugo Basile, Comerio-Varese, Italy) which generates a linearly increasing mechanical force. Briefly, a metal filament applied a linear increasing pressure under the plantar surface of the hind limb using an electronic Von Frey hair unit. The withdrawal threshold was measured by applying force ranging from 0 to 50 g within 20 s. Mechanical threshold reflex was measured automatically by the grams until withdrawal in response to the applied force. Two h after dynamic test, change in thermal hyperalgesia after single and chronical treatments of Bort were monitored using Plantar test (Hargreaves' method; Ugo Basile, Comerio-Varese, Italy), as described previously (1). Briefly, after habituation, a movable infrared heat source (IR 40) was located directly under the plantar surface on the hind paw, and withdrawal latency (s) was used for data analysis. Sensory conduction studies (sensory nerve action potential amplitude and nerve conduction velocity) of caudal and hind limb digital nerves (extensively used in the classification of peripheral neuropathies) were assessed orthodromically (2) through the Myto2 EGM device (EBN Neuro, Firenze, Italy). Briefly, the recordings were performed by placing the reference recording electrode and the active recording electrode at 1 and 2 cm from the base of the tail, the ground electrode at 2.5 cm from the base of the tail, and cathode and anode at 5 and 6 cm respectively. To study digital nerve, the cathode and the anode were placed at the base and at the tip of the fourth toe of the left hind-limb respectively, the ground electrode subcutaneously in the sole, and active recording electrode and reference recording electrode at the ankle and subcutaneously near the patellar bone, respectively. Intensity, duration and frequency of stimulation were set up in order to obtain supramaximal results. Animals were anesthetized with 2% isoflurane and the body temperature was kept constant at 37 ± 0.5 °C with a temperature-controlled heating pad operated via a thermal rectal probe (Harvard Apparatus, Holliston, US).

Quantitative immunoblotting and immunocytochemistry of tubulin PTMs and MT markers. Whole cell lysates from cultured DRG neurons were obtained by manual homogenization in Laemmli buffer 1x (62.5 mM Tris pH 6.8, 10% glycerol, 5% DTT, 2% SDS, 0.004% bromophenol blue) followed by sonication (Bransor-Sonifier 250 for 15 s), boiling (95 °C for 5 min) and pre-clearing (5 min at 10,000 x g). Proteins were separated by 10% Bis-Tris gel (Invitrogen) and transferred to nitrocellulose membrane. After blocking in 5% milk/TBS, membranes were incubated with primary antibodies at 4 °C overnight or 1 h at 37 °C and 1 h with secondary antibodies at R.T.. Secondary antibodies conjugated to IR680 or IR800 (Rockland Immunochemicals) were used for multiple infrared detection. Image acquisition was performed with an Odyssey imaging system (LI-COR Biosciences, NE) and analyzed with Odyssey software. For immunofluorescence (IF) studies of fixed tissue specimens, DRG and sciatic nerve sections were processed as follows: paraffin embedded blocks of DRG (L4-L5) and sciatic nerve samples were serially cut (5 µm) and deparaffinized by immersing the slices in xylene (7 min x 2) followed by 100%, 90%, 80%, 60%, 40% EtOH (5 min each) and H_2O (5 min) immersion. Slices were then rinsed with PBS 1x (10 min x 2) and antigen retrieval carried out by boiling the slices in citric acid solution (10 mM, pH 6) for 15 min. Sections

were cooled down for 15 min, rinsed 3 times with PBS 1x, permeabilized with 0.01% Triton X-100 for 10 min and blocked with NGS (Thermofisher) 10% in PBS for 1 h at R.T. Primary antibodies incubations were performed overnight at 4 °C in normal goat serum (NGS) 10% PBS 1x buffer. For IF studies of isolated DRG neurons, cells were fixed with 4% PFA for 10 min, followed by membrane permeabilization with 0.1% Triton X-100, blocking with NGS and then staining overnight with primary antibodies as previously described (3). Alexa Fluor fluorescent dyes-conjugated secondary antibodies were diluted 1:200 in 10% NGS-PBS 1x and added for 1 h at R.T.. Acquisition was performed using a spinning disk confocal microscope (Olympus DSU) coupled to a camera controller Hamatsu (C10600 ORCA-R^2) or epifluorescence microscopy (Olympus IX81) coupled to a monochrome CCD camera (Sensicam QE; Cooke Corporation) and all images were analyzed by ImageJ software. Ratiometric analyses of tubulin PTM/bulk tubulin levels on DRG cellular bodies, sciatic nerve and proximal and distal axons of cultured DRG neurons were performed using fluorescence intensity levels of primary antibodies on randomly selected cellular bodies, sciatic nerve or proximal axons (100 μm from the cell body) from images of fixed and immunostained specimens using ImageJ software.

Sural nerve biopsies and clinical history of control and BIPN patients. Clinical history of the BIPN patient shown was previously described (4). The patient was administered Bort 1.3 gm/m^2 and a second dose after 4 d to treat a marginal zone lymphoma. Neurological examination showed distal weakness, which was more severe in the legs, and sensory loss to pin, temperature and vibration distally in the hands and feet. An EMG and nerve conduction study showed signs of a sensorimotor neuropathy, with axonal loss and multifocal demyelination. The patient's sural nerve biopsy, performed 2 and ½ months after the second and last dose of Bort, showed a significant axonal loss involving both large and small myelinated fibers, with no robust axonal regeneration. There were scattered histiocytes/macrophages associated with active axonal breakdown in the nerve fascicles, along with perivascular T-cell-dominant lymphocytic inflammation. No overt vasculitis or amyloid deposition was seen. By teased fiber analysis, 22% of the teased myelinated fibers showed Wallerian degeneration and 22% showed myelin changes in the forms of segmental demyelination and remyelination. After stopping Bort, nerve conduction studies after 22 months showed improvement in the compound muscle action potential amplitudes. One control patient had a right sural nerve biopsy for a suspected mitochondrial disease (not specified). The morphology revealed a peripheral nerve with mild changes without significant inflammation, consisting of minimal axonal loss with 10% of the teased fibers exhibiting segmental remyelination. No amyloid deposition was observed. The second control patient was a suspected case of idiopathic peripheral neuropathy, not due to neurotoxic medications. The nerve biopsy, however, showed minimal changes that were indistinguishable from age-related alteration with minimal axonal loss and 9.3% of the teased fibers exhibiting segmental remyelination. No vasculitis, amyloidosis, and immunoglobulin deposition were detectable. The third control patient underwent a sural nerve biopsy with the symptoms of peripheral neuropathy, parkinsonism, bulbar palsy and history of Lyme disease. The sural nerve revealed minimal changes, without any significant axonal loss. By the nerve teasing, 11% of the fibers showed segmental remyelination. No vasculitis or amyloid deposition was identified. The sural nerve biopsies were performed as previously described (5).

Caspase cleavage assay. Caspase activation was assessed in DRG neurons treated with vehicle (DMSO) or 100 nM of Bortezomib up to 48 h using an *in vitro* caspase-3 like cleavage assay utilizing the chemical substrate DEVD-7-amino-4-methylcoumarin (AMC) (Enzo Life Sciences, Farmingdale, NY #ALX-260-031). At the end of treatment, AMC substrate was added to the wells and neurons were incubated for 30 min at 37 °C in the dark. The generation of the fluorescent AMC cleavage product was measured at 360 nm excitation and 460 nm emissions, using a fluorescence plate reader (SpectraMax i3x multi-mode detection platform, Molecular Devices). Addition of staurosporine at the concentration of 600 nM for 24 h was used as a positive control (6).

Fly stocks and *Drosophila* larval assays. *UAS-EB1-GFP* on III (BL 35512) and *477-Gal4* on II (BL 8737) (7) were obtained from the Bloomington Stock Center (Bloomington, IN). *ppk-CD4-tdGFP* (III) has been described previously (8). Bort (LC laboratories) was diluted to 2.5 mM in ethanol, aliquoted and stored in -80 °C until use. Fresh aliquots of Bort were diluted to a final concentration of 20 μM in 1x PBS. A matching concentration of ethanol was added as a vehicle control. This solution was used to make food using instant *Drosophila* medium (Formula 4-24 ®, Carolina Biological Supply Company) immediately before starting the larval assay in 1:1 (vol/vol). Embryos were collected on grape plates with yeast paste made with 0.5 %

propionic acid. For acute treatment (3 h and 6 h) for live imaging of EB1, third instar larvae were collected. For chronic treatment, first instar larvae (24-28 h after egg laying) were collected manually with a paintbrush. All collected larvae were washed in 1 × PBS and placed into either Bort or vehicle-containing food. All larvae were reared at 22-25° C. For acute treatment, 2-3 similarly sized larvae from control and Bort treated larvae were collected from each experiment. For chronic treatment larvae were stage-matched to late third instar (based on the morphology of anterior spiracles) at the time of collection. Controls typically reached late third instar by 5-7 d. Any remaining animals that did not reach late third instar by 10 d after starting the treatment were discarded. All animals matching the developmental criteria were collected to avoid any selection bias.

Degeneration index in sensory neurons of *Drosophila* larvae. Immunolabeling of *Drosophila* larvae was performed largely as described previously (9). Briefly, late third instar larvae were dissected in 1 × PBS, fixed in 4% paraformaldehyde (PFA, Electron Microscopy Sciences) in 1 × PBS for 15 min, rinsed three times in 1 × PBS + 0.3% Triton X-100 (PBS-TX), and blocked for 1 h at R.T. or overnight at 4 °C in 5% normal donkey serum (NDS) in PBS-TX (Jackson ImmunoResearch). Primary antibodies were chicken anti-GFP (1:1000; Abcam) diluted in 5% NDS in PBS-TX. Tissue was incubated overnight in primary antibodies at 4 °C and then washed in PBS-TX for 3 × 15 min at R.T.. Species-specific, fluorophore-conjugated secondary antibodies (Jackson ImmunoResearch) were used at 1:1000 in 5% NDS in PBS-TX, and incubated overnight 4 °C. Tissue was rinsed in PBS-TX for 3 × 15 min with a final rinse in PBS. Tissue was mounted on poly-L-lysine coated coverslips, dehydrated 5 min each in an ascending ethanol series (30, 50, 70, 95, 2 × 100%), cleared in xylenes (2 × 10 min), and mounted in DPX (Fluka). *Drosophila* sensory neurons were imaged on a Zeiss 510 Meta laser scanning confocal microscope (25x objective, glycerol, 1.4 NA, Plan-Neofluar). Entire body walls were imaged in tiles, and then stitched using Grid/Collection stitching plugin in Fiji software (10) to capture all ddaC nociceptive neurons in abdominal segments in each animal. All images were randomized and blinded before single cells were cropped out for further analysis. Images containing single cells were batch processed using automatic global threshold (default method), made binary, and the particle analyzer plugins of Fiji was used to calculate degeneration index as described previously in the neurodegeneration index measurements of DRG neurons (11).

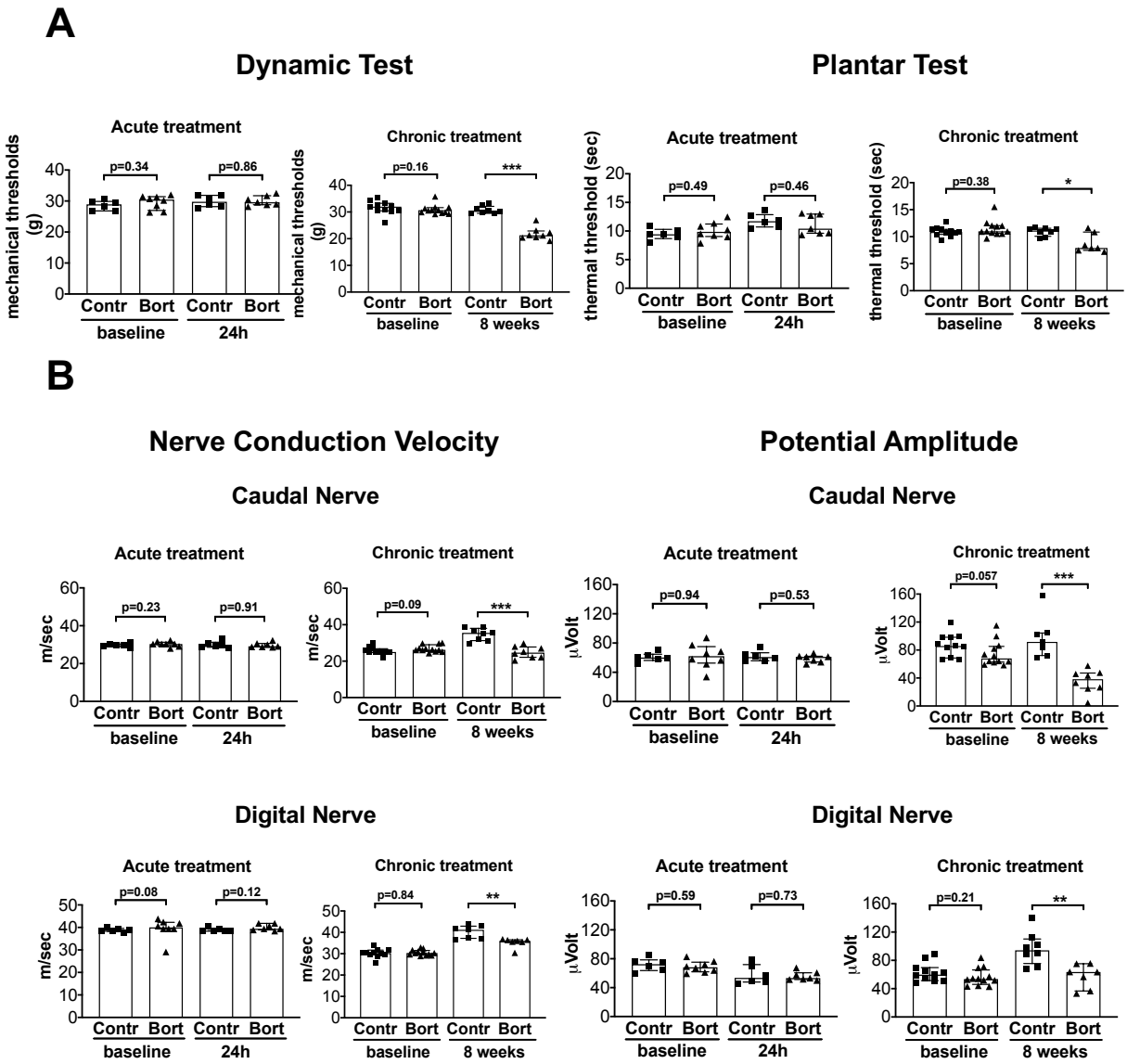

Fig. S1. Behavioral tests and neurophysiological studies in control and bortezomib-treated rats after 24 h or 8 wk of treatment. (A) Hind-paw withdrawal response to mechanical stimulus (Dynamic Test) and plantar withdrawal latency response to heat source (Plantar Test) were recorded before chemotherapy administration (baseline value), after 24 h and at the end of treatment (8 wk) with bortezomib (Bort). Mechanical allodynia and thermal hyperalgesia were observed only at the end of chronic administration of Bort in treated animals (Bort) compared to controls (Contr). (B) Digital and caudal nerve conduction velocity (NCV) and amplitude were measured before chemotherapy administration (baseline value), after 24 h and at the end of treatment (8 wk) with Bort. Only after 8 w of treatment with Bort significant decrease of caudal and digital NCV and potential amplitude were evident in treated rats vs controls (Contr). Data are expressed as medians plus interquartile range and analyzed by Mann-Whitney test, n=6-13 animals per condition.

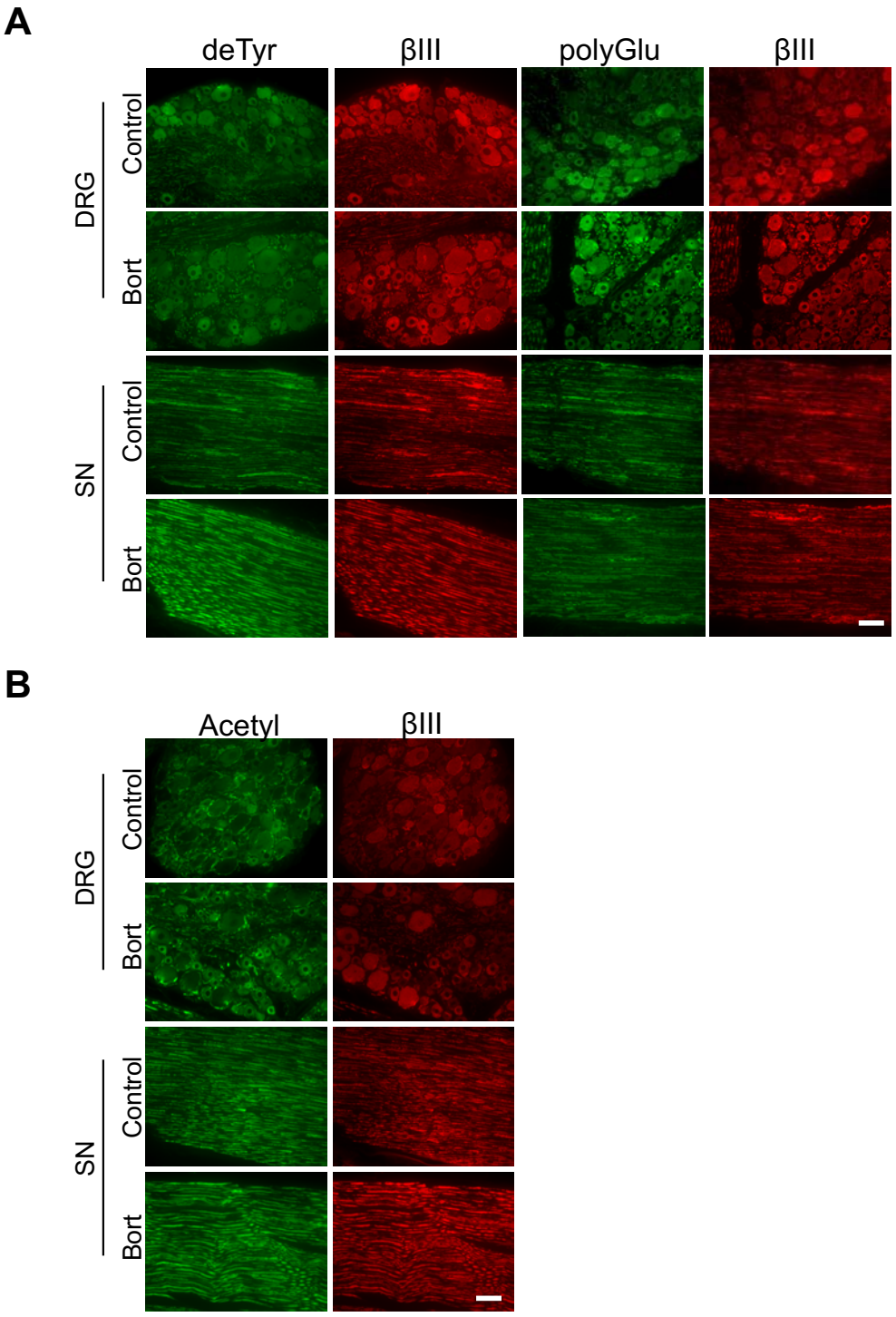

Fig. S2. De-tyrosinated, acetylated and polyglutamylated tubulins in rats treated with acute doses of bortezomib. (A, B) Representative tubulin PTM immunofluorescence staining of dorsal root ganglia (DRG) cell bodies and sciatic nerve (SN) isolated from rats acutely treated with bortezomib (Bort) as in Fig. 1B. DeTyr, de-tyrosinated tubulin; polyGlu polyglutamylated tubulin (GT335); Acetyl, acetylated tubulin; βIII, βIII tubulin. Scale bar, 20 μm.

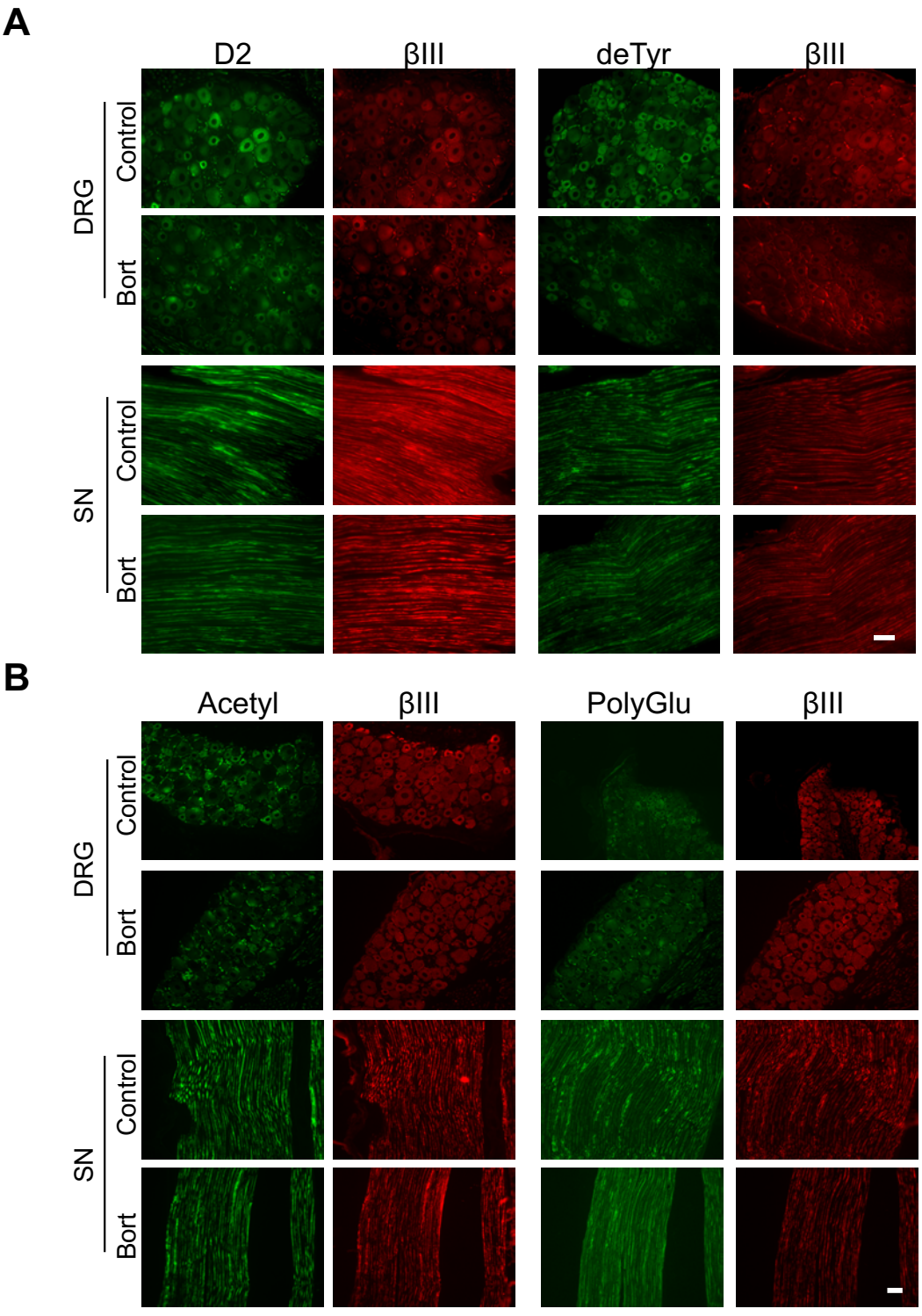

Fig. S3. D2, De-tyrosinated, acetylated and polyglutamylated tubulins in rats treated with chronic doses of bortezomib. (A, B) Representative tubulin PTM immunofluorescence staining of DRG cell bodies and sciatic nerve (SN) isolated from rats chronically treated with bortezomib (Bort) as in Fig. 1C. D2, delta 2 tubulin; deTyr, de-tyrosinated tubulin; polyGlu, polyglutamylated tubulin (GT335); Acetyl, acetylated tubulin; βIII, βIII tubulin. Scale bar, 50 μm.

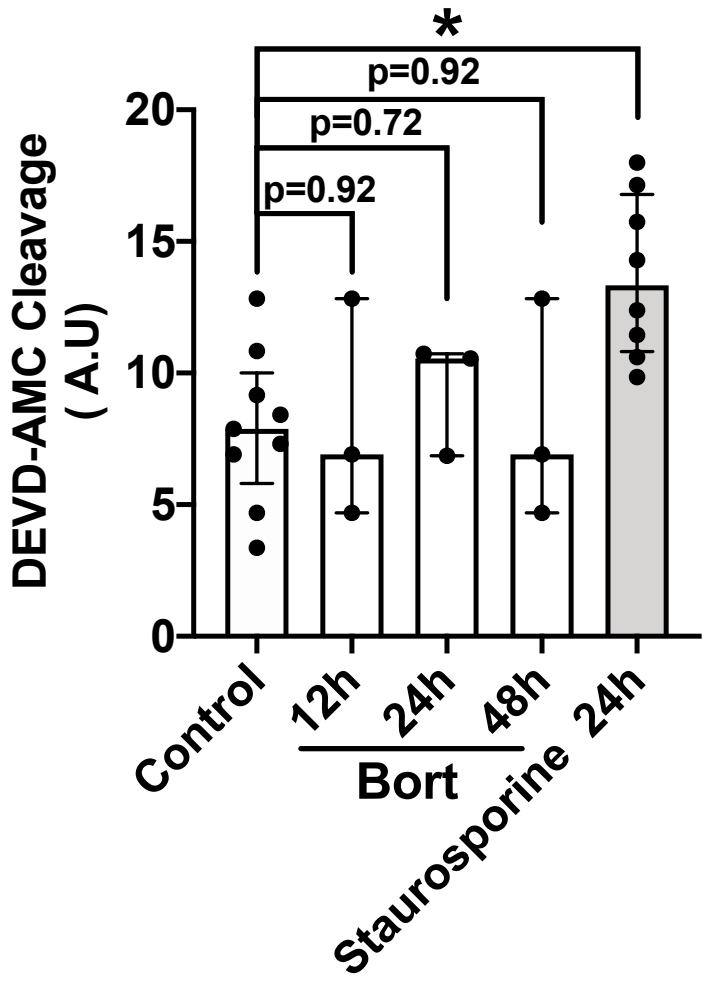

Fig. S4. Bortezomib does not increase caspase-3 enzymatic activity in cultured DRG neurons at the onset of axonal degeneration. Caspase-3 enzymatic activity was measured in DRG neurons plated on 96 well dishes and treated with 100 nM bortezomib (Bort) at the concentration for indicated times. Staurosporine (600 nM) was added for 24 h as a positive control. Data are reported as medians plus interquartile range, (n=3 triplicates; 3-9 wells per condition) and analyzed by Kruskal-Wallis test.

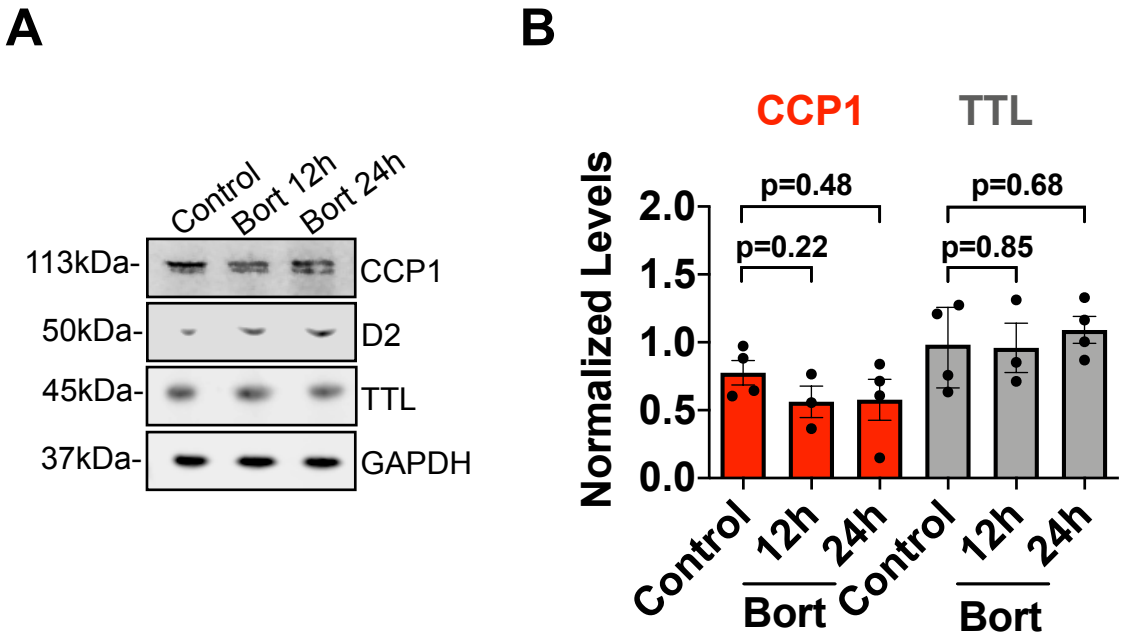

Fig. S5. CCP1 and TTL levels are not affected by bortezomib at onset of neurodegeneration. (A) Immunoblot analyses of carboxypeptidase 1 (CCP1), tubulin tyrosine ligase (TTL) and D2 levels in whole cell lysates from DRG neurons (12 DIV) treated with DMSO (Control) or 100 nM for the indicated times. (B) Quantification of GAPDH normalized CCP1 and TTL levels as in A. Data are shown as medians plus interquartile range and analyzed by Mann-Whitney test.

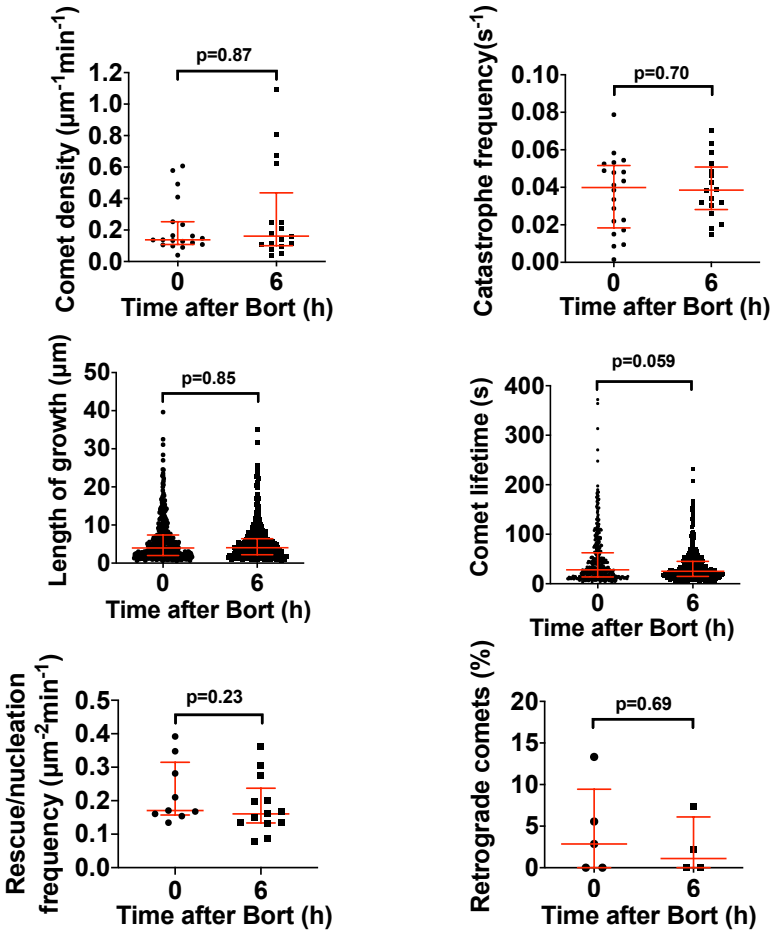

Fig. S6. Additional MT dynamics parameters in the peripheral nerve fibers of zebrafish exposed to bortezomib. MT dynamics parameters in the peripheral nerve fibers of zebrafish treated as in Fig 4B. Data were pooled from 3 individual fish containing 4 to 5 neurites with up to 80-220 comets and analyzed by Mann-Whitney test. Data are shown as median plus interquartile range.

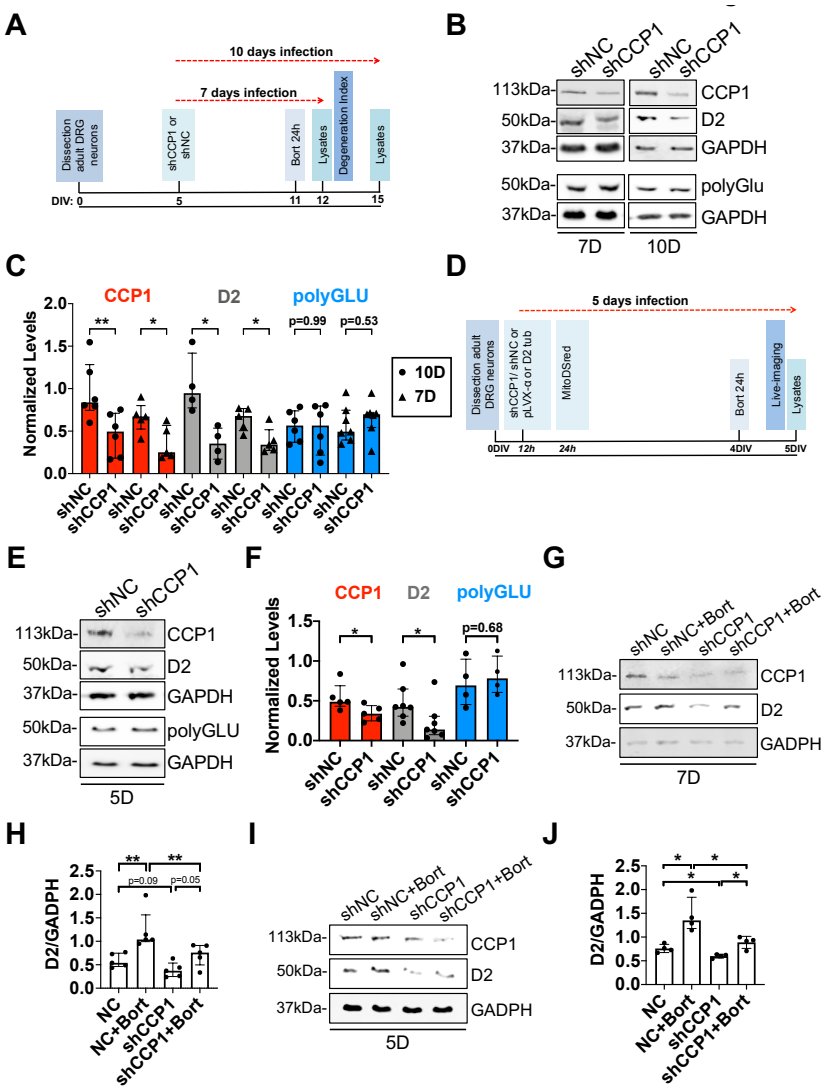

Figure S7. CCP1 depletion affects D2 levels. (A) Schematic of the experimental strategy for 7 and 10 d infection to analyze axonal degeneration as in Fig. 6. (B) Immunoblot analyses of CCP1, D2 and polyglutamylated tubulin levels from whole cell lysates of DRG neurons infected for 7 or 10 d with shCCP1 or shNC lentivirus. (C) Quantification of normalized CCP1, D2 and polyglutamylated tubulin levels as in B. Data are pooled from 4-7 experiments. (D) Schematic of the 5 d infection strategy with shCCP1 or shNC lentivirus and pLVX-EGFP-D2- or WT-α-tubulin lentivirus to analyze mitochondria motility as in Fig. 7. (E) Immunoblot analyses of CCP1, D2 and polyglutamylated tubulin levels of whole cell lysates of DRG neurons infected for 5 d with shCCP1 or shNC lentivirus. (F) Quantification of normalized CCP1, D2 and polyglutamylated tubulin levels as in E. Data are pooled from 5-7 experiments. (G) Immunoblot analyses of CCP1 and D2 levels of whole cell lysates of DRG neurons infected for 7 d with shCCP1 or shNC lentivirus plus and minus bortezomib (Bort) as in Fig. 6. (H) Quantification of normalized D2 levels as in G. Data are pooled from 5 experiments. (I) Immunoblot analyses of CCP1 and D2 levels of whole cell lysates of DRG neurons infected for 5 d with shCCP1 or shNC lentivirus plus and minus bortezomib (Bort) as in Fig. 7. (J) Quantification of normalized D2 levels as in I. Data are pooled from 4 experiments. PolyGlu, polyglutamylated tubulin (polyE); GAPDH, loading control. All data in C, F, H and J are shown as medians plus interquartile range and statistics analyzed by Mann-Whitney test.

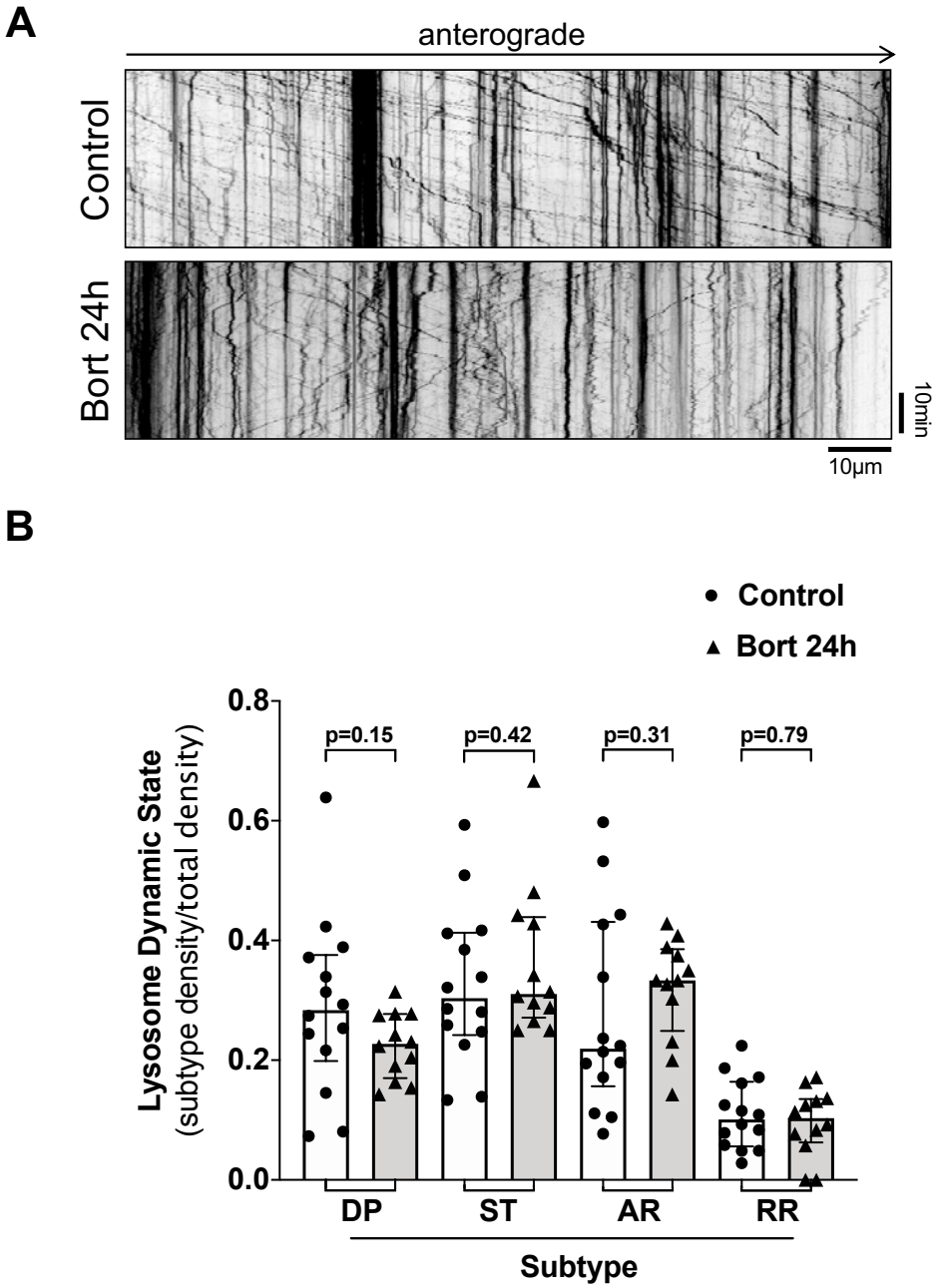

Fig. S8. Bortezomib does not affect lysosome motility in DRG neurons at the onset of neurodegeneration. (A) Representative kymographs of lysosome movement in DRG neurons (5 DIV) infected at 1 DIV with Lamp1-mRFP-FLAG lentivirus followed by bortezomib (Bort) treatment (100 nM for 24 h). Videos (10s/frame for 30 min). Scale bar, 10 μm. (B) Quantification of lysosome dynamic states, Dynamic Pause (DP), Stationary (ST), Anterograde Running (AR), Retrograde Running (RR), in DRG neurons treated as in A. Data are shown as medians plus interquartile range from 12-15 neurites and analyzed by Mann-Whitney test.

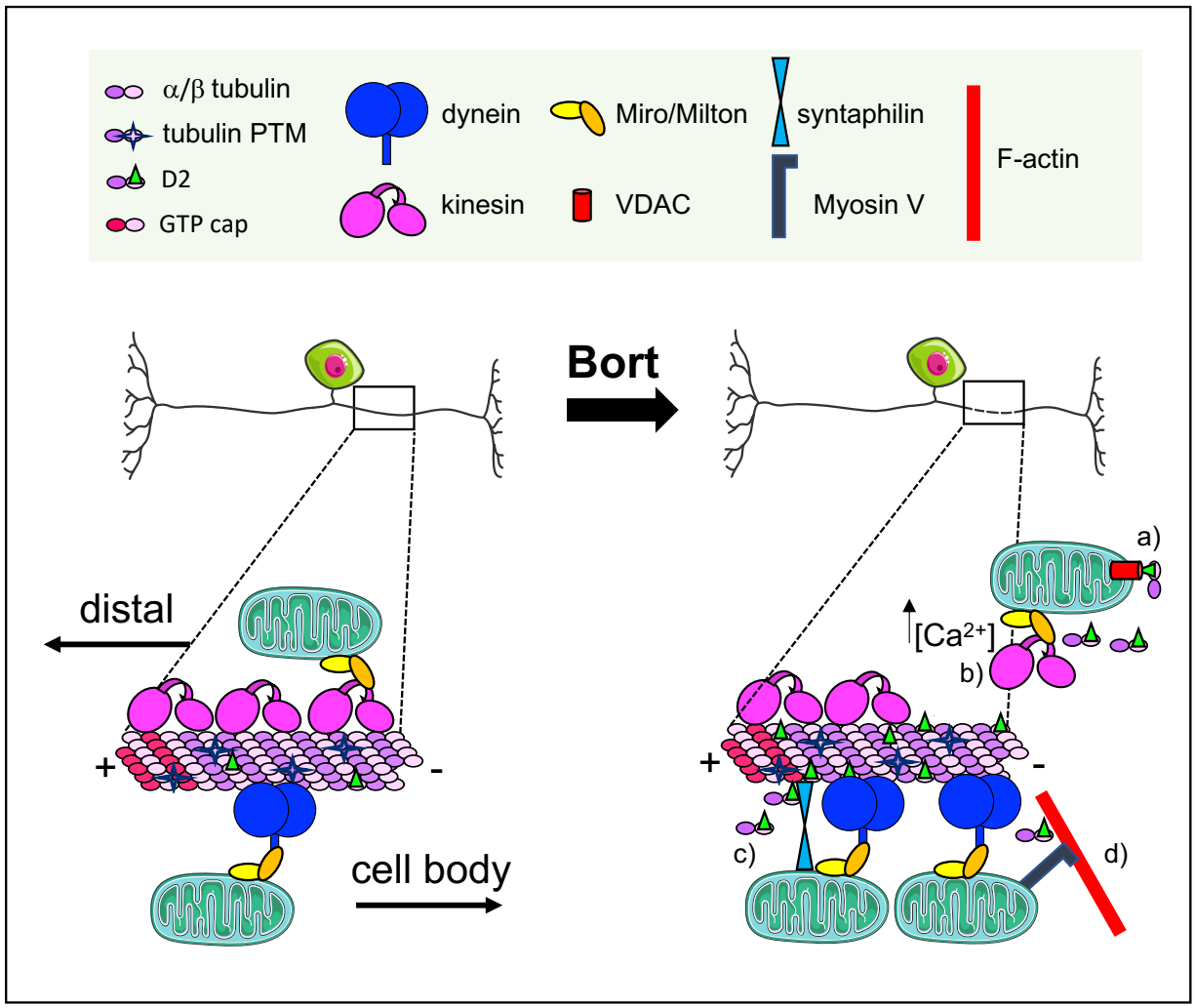

Fig. S9. Proposed pathogenic role of D2 in BIPN. Bortezomib exposure promotes premature tubulin longevity and D2 accumulation at a prodromal stage of the disease. Soluble D2 accumulation may induce axonal degeneration by selective inhibition of mitochondria motility that might occur through at least four non mutually exclusive modalities: a) by interfering with mitochondria bioenergetics through direct D2 binding to the VDAC; b) by raising intracellular Ca^{2+} levels causing Miro-dependent mitochondria/motor complex detachment from MTs; c,d) by increasing the affinity of the anchoring proteins Syntaphilin (c) or Myosin V (d) to mitochondria and either MTs (c) or F-actin (d).

Figure 1							
	DRG	**Control vs Bort**	**D2 vsPTMs**	**SN**	**Control vs Bort**		**D2 vs PTMs**
Panel B	***Acute Treatment in Rat***	*pValue*	*pValue*	***Acute Treatment***	*pValue*		*pValue*
IF	*D2*	*0.004*		*D2*	*0.02*		
	Acetylated	*0.99*	*0.03*	*Acetylated*	*0.99*		*0.22*
	PolyGlu	*0.62*	*0.01*	*PolyGlu*	*0.22*		*0.02*
	deTyr	*0.4*	*0.01*	*deTyr*	*0.3*		*0.62*
Panel C	***Chronic Treatment in Rat***	*pValue*	*pValue*	***Chronic Treatment***	*pValue*		*pValue*
IF	*D2*	*0.02*		*D2*	*0.34*		
	Acetylated	*0.2*	*0.057*	*Acetylated*	*0.057*		*0.057*
	PolyGlu	*0.11*	*0.9*	*PolyGlu*	*0.88*		*0.88*
	deTyr	*0.02*	*0.02*	*deTyr*	*0.99*		*0.48*
Panel E	***Acute Treatment in Rat***	*pValue*					
IF	Peripherin neurons positive to D2	*0.01*					
	NF200 neurons positive to D2	*0.11*					
	Peripherin vs NF200	*0.002*					
Panel G	***Sural Nerve Biopsy in Human***	***Patient 1 vs Patient 4***	***Patient 2 vs Patient 4***	***Patient 3 vs Patient 4***			
IF		*pValue*	*pValue*	*pValue*			
	D2	*0.004*	*0.009*	*0.009*			
Figure 1S	***Acute Treatment in Rat***	Baseline	24h	***Chronic Treatment***	Baseline		*8w*
Panel A	***Behavioural Test***	*Control vs Bort*	*Control vs Bort*	***Behavioural Test***	*Control vs Bort*		*Control vs Bort*
		pValue	*pValue*		*pValue*		*pValue*
	Dynamic Test	*0.34*	*0.86*	*Dynamic Test*	*0.16*		*0.0002*
	Plantar Test	*0.49*	*0.46*	*Plantar Test*	*0.38*		*0.02*
Panel B	***Electrophysiology***	*pValue*	*pValue*	***Electrophysiology***	*pValue*		*pValue*
	Caudal Nerve conduction velocity	*0.23*	*0.91*	*Caudal Nerve Conduction Velocity*	*0.09*		*0.0003*
	Digitall Nerve conduction velocity	*0.08*	*0.12*	*Digital Nerve conduction velocity*	*0.84*		*0.002*
	Potential Amplitude Caudal Nerve	*0.94*	*0.53*	*Potential Amplitude Caudal Nerve*	*0.057*		*0.0003*
	Potential Amplitude Digital Nerve	*0.59*	*0.73*	*Potential Amplitude Digital Nerve*	*0.21*		*0.003*
Figure 2							
Panel B	***In vitro DRG neurons***		***100nM Bort***				
IF		*Control vs 6h*	*Control vs 12h*	*Control vs 24h*			
		pValue	*pValue*	*pValue*			
	D2/βIII	*0.63*	*0.02*	*0.002*			
Panel C	***In vitro DRG neurons***		*100nM Bort*				
Degeneration Index		*Control vs 6h*	*Control vs 12h*	*Control vs 24h*	*Control vs 48h*		*Control 72h*
		pValue	*pValue*	*pValue*	*pValue*		*pValue*
	Neurofilament	*0.41*	*0.07*	*0.03*	*0.03*		*0.03*
Panel E	***In vitro DRG neurons***		*100nM Bort*				
IB		*Control vs 24h*	*Control 48h*	*Control vs 72h*			
		pValue	*pValue*	*pValue*			
	D2	*0.01*	*0.004*	*0.004*			
Panel G	***In vitro DRG neurons***		***100nM Bort***				
IB	*Soluble tub/MT pellet*	*Control vs 12h*	*Control 24h*	*Control vs 48h*			
		pValue	*pValue*	*pValue*			
	D2	*0.53*	*0.16*	*0.02*			
	βIII	*0.9*	*0.3*	*0.15*			
Figure 3							
Panel B	***In vitro DRG neurons***		***100nM Bort***				
Stability Assay		*Contr vs Contr+NZ*	*3h vs 3h +NZ*	*6h vs 6h +NZ*	*Control vs 3h*	*Control vs 6h*	*3h vs 6h*
		pValue	*pValue*	*pValue*	*pValue*	*pValue*	*pValue*
IF	*βIII*	*<0.0001*	*<0.0001*	*0.14*	*0.99*	*0.8*	*0.57*
Panel D	***In vitro DRG neurons***		***100nM Bort***				
		Control vs 2h	*Contr vs 3h*	*Control vs 6h*			
		pValue	*pValue*	*pValue*			
IB	*Acetlated*	*0.34*	*0.02*	*0.0006*			
	deTYR	*0.99*	*0.39*	*0.01*			
Panel F	***In vitro DRG neurons***		***100nM Bort***				
MT Dynamics		*Control vs 1h*	*Control vs 2h*	*Control vs 3h*	*Control vs 6h*		*Control vs 24h*
		pValue	*pValue*	*pValue*	*pValue*		*pValue*
	Growth rate	*< 0.0001*	*< 0.0001*	*< 0.0001*	*< 0.0001*		*< 0.0001*
	Comet density	*0.001*	*0.004*	*< 0.0001*	*< 0.0001*		*0.002*
	Catastrophe frequency	*0.009*	*0.17*	*0.002*	*0.0008*		*0.17*
	Length of growth	*0.55*	*0.08*	*0.22*	*< 0.0001*		*0.002*
	Comet life time	*< 0.0001*	*< 0.0001*	*< 0.0001*	*< 0.0001*		*0.001*
	Rescue or nucleation	*0.0008*	*0.001*	*< 0.0001*	*< 0.0001*		*0.0005*
Figure 4							
Panel C	***In vivo in Zebrafish***	**1.3 uM Bort**	**Panel G**	***In vivo in Drosophila***	**20 uM Bort**		
MT Dynamics		*Control vs 6h*		*Control vs 3h*	*Control vs 6h*		*3h vs 6h*
		pValue		*pValue*	*pValue*		*pValue*
	Growth rate	*< 0.0001*	*Growth rate*	*0.27*	*0.001*		*0.006*
Figure S6	*Comet density*	*0.87*	*Comet density*	*0.03*	*0.04*		*0.46*
	Catastrophe frequency	*0.7*	*Catastrophe frequency*	*< 0.0001*	*< 0.0001*		*0.3*
	Length of growth	*0.85*	*Length of growth*	*< 0.0001*	*< 0.0001*		*0.0002*
	Comet life time	*0.059*	*Comet life time*	*< 0.0001*	*< 0.0001*		*0.07*
	Rescue or nucleation	*0.23*	*Rescue or nucleation*	*0.02*	*0.09*		*0.28*
	Retrograde comets	*0.69*	**Panel E**	*Control vs Bort*			
			Degeneration Index	*0.04*			
Figure 5							
Panel D	***In vitro DRG neurons***		***Lentiviral shRNA Delivery***	**PanelG**			
Degeneration Index		*shNC vs shTTL1*	*shNC vs shTTL2*	*No Virus vs pLVX-EGFP-WT tub*	*No Virus vs pLVX-EGFP-WT tub*		
		pValue	*pValue*	*pValue*	*pValue*		
	Neurofilament	*0.01*	*0.007*	*0.28*	*0.009*		
Figure 6			***Lentiviral shRNA Delivery (7D)***				
Panel B	*In vitro DRG neurons*	*shNC vs shNC+Bort*	*shCCP1 vs shCCP1+Bort*	*shNC+Bort vs shCCP1+Bort*			
Degeneration Index	Neurofilament	*0.02*	*0.57*	*0.02*			
Figure 7			***Lentiviral shRNA Delivery (5D)***				
Panel B	***In vitro DRG neurons***	*shNC vs shNC+Bort*	*shCCP1+shCCP1+Bort*	*shNC+Bort vs shCCP1+Bort*			
		pValue	*pValue*	*pValue*			
Mitochondria Dynamics	*DP*	*0.41*	*< 0.0001*	*0.09*			
	ST	*<0.0001*	*0.31*	*< 0.0001*			
	AR	*< 0.0001*	*0.0001*	*< 0.0001*			
	RR	*< 0.0001*	*0.001*	*0.0007*			
Panel D	***In vitro DRG neurons***	*No Virus vs pLVX-EGFP-WT tub*	*No Virus vs pLVX-EGFP-D2*	*pLVX-EGFP-WT tub vs pLVX-EGFP-D2*			
		pValue	*pValue*	*pValue*			
Mitochondria Dynamics State	*DP*	*0.056*	*0.87*	*0.09*			
	ST	*0.81*	*< 0.0001*	*< 0.0001*			
	AR	*0.22*	*< 0.0001*	*< 0.0001*			
	RR	*0.94*	*< 0.0001*	*< 0.0001*			
Figure S4							
	In vitro DRG neurons		***100nM Bort***		*Staurosporine*		
		Contr vs 12h	*Contr vs 24h*	*Contr vs 48h*	*Contr vs 24h*		
caspase activity		*pValue*	*pValue*	*pValue*	*pValue*		
	DEVD-AMC cleavage	*0.92*	*0.72*	*0.92*	*0.02*		
Figure S5				**Figure S8**			
Panel B	*In vitro DRG neurons*	*100nM Bort*		**Panel B**	*100nM*		
		Contr vs 12h	*contr vs 24h*		*Contr vs Bort*		
		pValue	*pValue*				*pValue*
IB	*CCP1*	*0.22*	*0.48*				
	TTL	*0.85*	*0.68*	**Lysosome Dynamics State**	*DP*		*0.15*
					ST		*0.42*
					AR		*0.31*
					RR		*0.79*
Figura S7	*In vitro DRG neurons*		***Lentiviral shRNA Delivery***				
			shNC vs ShCCP1				
Panel C and F		***5D (Panel F)***	***7D (Panel C)***	***10D (Panel C)***			
		pValue	*pValue*	*pValue*			
IB	*D2*	*0.03*	*0.008*	*0.03*			
	CCP1	*0.02*	*0.02*	*0.03*			
	polyGLU	*0.68*	*0.99*	*0.53*			
		shNC vs shNC+Bort	*shCCP1 vs shCCP1+Bort*	*shNC+Bort vs shCCP1+Bort*	*shNC vs shCCP1*		
		pValue	*pValue*	*pValue*	*pValue*		
Panel H	**7D**	*0.079*	*0.055*	*0.079*	*0.09*		
IB	*D2*						
Panel E	**5D**						
IB	D2	*0.02*	*0.02*	*0.02*	*0.02*		

Table S1. Table showing p values derived from statistical analysis of quantitative data included in Figures and Supplementary Figures.

Supplementary Movies

Movie S1. EB3-EGFP dynamics in axons of cultured mouse DRG neurons treated 0 h with bortezomib (Figure 3E).

Movie S2. EB3-EGFP dynamics in axons of cultured mouse DRG neurons treated 6 h with bortezomib (Figure 3E).

Movie S3. EB3-GFP dynamics in adult zebrafish skin nerve endings treated 0 h with bortezomib (Figure 4B).

Movie S4. EB3-GFP dynamics in adult zebrafish skin nerve endings treated 6 h with bortezomib (Figure 4B).

Movie S5. EB1-GFP dynamics in a nociceptive neuron of third star *Drosophila* larva treated with vehicle control (Figure 4F).

Movie S6. EB1-GFP dynamics in a nociceptive neuron of third star *Drosophila* larva treated 6 h with bortezomib (Figure 4F).

Movie S7. LAMP1- mRFP-FLAG dynamics in axons of untreated cultured mouse DRG neurons (SI Appendix, Figure S8A).

Movie S8. LAMP1- mRFP-FLAG dynamics in axons of cultured mouse DRG neurons treated with 100 nM Bort (24 h) (SI Appendix, Figure S8A).

Movie S9. Mito-dsRed dynamics in axons of cultured mouse DRG neurons infected with control shNC lentivirus (Figure 7A).

Movie S10. Mito-dsRed dynamics in axons of cultured mouse DRG neurons infected with control shNC lentivirus plus 100 nM Bort (24 h) (Figure 7A).

Movie S11. Mito-dsRed dynamics in axons of cultured mouse DRG neurons infected with shCCP1 lentivirus (Figure 7A).

Movie S12. Mito-dsRed dynamics in axons of cultured mouse DRG neurons infected with shCCP1 lentivirus plus 100 nM Bort (24 h) (Figure 7A).

Movie S13. Mito-dsRed dynamics in axons of non-infected cultured mouse DRG neurons (Figure 7C).

Movie S14. Mito-dsRed dynamics in axons cultured mouse DRG neurons infected with control EGFP-α-tub lentivirus (Figure 7C).

Movie S15. Mito-dsRed dynamics in axons of cultured mouse DRG neurons infected with EGFP-D2-tub lentivirus (Figure 7C).

SI References

1. C. Meregalli *et al.*, CR4056, a new analgesic I2 ligand, is highly effective against bortezomib-induced painful neuropathy in rats. *J Pain Res* **5**, 151-167 (2012).
2. J. P. Rasmussen, N. T. Vo, A. Sagasti, Fish Scales Dictate the Pattern of Adult Skin Innervation and Vascularization. *Dev Cell* **46**, 344-359 e344 (2018).
3. X. Qu *et al.*, Stabilization of dynamic microtubules by mDia1 drives Tau-dependent Abeta1-42 synaptotoxicity. *J Cell Biol* **216**, 3161-3178 (2017).
4. S. P. Thawani, K. Tanji, E. A. De Sousa, L. H. Weimer, T. H. Brannagan, 3rd, Bortezomib-associated demyelinating neuropathy--clinical and pathologic features. *J Clin Neuromuscul Dis* **16**, 202-209 (2015).
5. C. B. Mikell, A. K. Chan, G. E. Stein, K. Tanji, C. J. Winfree, Muscle and nerve biopsies: techniques for the neurologist and neurosurgeon. *Clin Neurol Neurosurg* **115**, 1206-1214 (2013).
6. E. Bianchetti, S. J. Bates, S. L. Carroll, M. D. Siegelin, K. A. Roth, Usp9X Regulates Cell Death in Malignant Peripheral Nerve Sheath Tumors. *Sci Rep* **8**, 17390 (2018).
7. W. B. Grueber, L. Y. Jan, Y. N. Jan, Different levels of the homeodomain protein cut regulate distinct dendrite branching patterns of Drosophila multidendritic neurons. *Cell* **112**, 805-818 (2003).
8. C. Han, L. Y. Jan, Y. N. Jan, Enhancer-driven membrane markers for analysis of nonautonomous mechanisms reveal neuron-glia interactions in Drosophila. *Proc Natl Acad Sci U S A* **108**, 9673-9678 (2011).
9. B. J. Matthews *et al.*, Dendrite self-avoidance is controlled by Dscam. *Cell* **129**, 593-604 (2007).
10. S. Preibisch, S. Saalfeld, P. Tomancak, Globally optimal stitching of tiled 3D microscopic image acquisitions. *Bioinformatics* **25**, 1463-1465 (2009).
11. J. Gerdts, Y. Sasaki, B. Vohra, J. Marasa, J. Milbrandt, Image-based screening identifies novel roles for IkappaB kinase and glycogen synthase kinase 3 in axonal degeneration. *J Biol Chem* **286**, 28011-28018 (2011).